Journal of Experimental and Applied Physics
Journal Homepage: jeap.ppj.unp.ac.id
Vol. 2, No. 1, March 2024.
ISSN (Print): 2988-0378 ISSN (Online): 2987-9256

Analysis of Lattice Constant, Structure and Crystal Size of TiO_2/Rough Bamboo Acitivated Carbon Nanocomposite for Battery Application

Zudiya Hifzi[1], Yenni Darvina[1*], Ramli[1], Ratnawulan[1], Fadhila Ulfa Jhora[1]

[1] Department of Physics, Universitas Negeri Padang, Padang 25131, Indonesia

Article History
Received : February, 9th 2024
Revised : February, 25th 2024
Accepted : March, 31st 2024
Published : March, 31st 2024

DOI:
https://doi.org/10.24036/jeap.v2i1.41

Corresponding Author
*Author Name: Yenni Darvina
Email: ydarvina@fmipa.unp.ac.id

Abstract: The working indicator of the battery is energy storage capacity, which depends on anode material. Generally, battery anodes are made from graphite but have limited energy capacity, which causes frequent overheating. One of the factors that influences energy storage capacity is surface area of the anode, where the smaller the particle size, the greater the storage capacity. So, research was carried out on materials that could replace graphite as an anode material for rechargeable batteries by having superior properties. This material is TiO_2/Rough bamboo activated carbon nanocomposite. Nanocomposites will be synthesized using the sol-gel method and then analyzed using XRD to obtain information about lattice constants, structure, and crystal size. So, this research aims to determine the lattice constant, structure, and crystal size of the forming materials such as carbon, activated carbon and TiO_2, and the TiO_2/Activated carbon nanocomposite. Nanocomposites will be synthesized with mass variations to see the superior properties of the two forming materials. Variations were carried out with mass ratios of TiO_2 and activated carbon, respectively, namely 40%:60%, 50%:50%, and 60%:40%. This research shows that the lattice constant in each variation has results that are by the shape of the crystal structure, and the crystal size value of the nanocomposite has reached the requirements as a nanocomposite material, namely a size below 100 nm. Activated carbon appears to have superior properties for smaller particle sizes than TiO_2.

Keywords: Crystal Size; Crystal Structure; Lattice Constants; Nanocomposites; XRD.

Journal of Experimental and Applied Physics is an open access article licensed under a Creative Commons Attribution ShareAlike 4.0 International License which permits unrestricted use, distribution, and reproduction in any medium, provided the original work is properly cited. ©2023 by author.

1. Introduction

Batteries are one of the most reliable sources of electrical energy to operate portable electronic equipment, such as cameras, cellphones, laptops, and others [1,2]. Rechargeable

How to cite:
Z. Hifzi, Y. Darvina, Ramli, Ratnawulan, and F. U. Jhora, 2024, Analysis of Lattice Constant, Structure and Crystal Size of TiO2/Rough Bamboo Acitivated Carbon Nanocomposite for Battery Application, *Journal of Experimental and Applied Physics,* Vol.1, No.1, page 1-16.

batteries are one of the most frequently used electrical energy storage materials because they have long durability and a long life cycle [3–5]. This batteries have excellent power and energy, so they are capable of stable charging. The advantages of the battery system are simple and practical, so this can be easy to use.

Rechargeable batteries can convert chemical energy into electrical energy by utilizing the reduction oxidation electrochemical reaction process. This batteries are comprise by anode, cathode, electrolyte, and separator [4]. The working indicator of a battery is its energy storage capacity, which depends on the anode material [6,7], and also has high stability [8]. Generally, graphite-based anodes have limited storage capacity [8] and often overheat [9], affecting the rechargeable battery's quality.

Previous research has synthesized Carbon-TiO_2 nanocomposites-as a lithium battery anode carried out by Aflahannisa & Astuti. In this research, it was found that the nanocomposite could overcome the problem of rechargeable battery anodes [6]. So, one effort that can be made to overcome this problem is to apply *Titanium dioxide* (TiO_2) as an energy storage material [10] to replace graphite because it has sufficient conductivity to overcome overheating problems in batteries. TiO_2 is a semiconductor material that meets the characteristics of an energy storage material because it can store energy [11], has good charge transfer, and has electrical properties [12]. The electrical conductivity of TiO_2 is $6{,}03\times10^{-3}$ S/m and can fix this problem. However, TiO_2 only has a theoretical capacity of 335 mAh/g, while graphite has a capacity of 372 mAh/g [6]. It can be overcome by adding other materials that can increase the energy capacity of the material so that the quality material with superior properties can be obtained. The TiO_2 material can be doped with other materials, such as activated carbon, to obtain superior material properties.

Activated carbon can be applied as an energy storage material. It meets the characteristics of being used as an anode for rechargeable batteries because it has a large energy capacity and can store and release a reasonable charge [4]. Activated carbon is a porous solid that contains 85% - 95% carbon and has pores in each particle because it has been heated to a high temperature [13]. Activated carbon has a greater energy capacity than graphite, namely 600 mAh/g [14]. Activated carbon that has gone through a carbonization and activation process will have good absorption in absorbing energy [15]. Research carried out by Taspika in 2015 [16] produced candlenut shell-activated carbon, which was then developed by Negara and Astuti (2015) into a battery anode material. This material produces a maximum electrical conductivity of $1{,}085\times10^{-4}$ S/m and a capacitance of 198,6 μF [16,17]. Susana & Astuti (2016) conducted research on the effect of LiOH concentration on the electrical properties of rechargeable battery anodes based on candlenut shell activated carbon, which resulted in an electrical conductivity of $2{,}34\times10^{-6}$ S/m and a capacitance of 327,93 μF [18]. Based on the research that has been carried out, activated carbon can be applied as an energy storage material.

Indonesia is a country that produces quite large natural materials [19]. One of the materials produced by nature in Indonesia is Rough Bamboo/Betung Bamboo (*Dendrocallamus asper*). This plant often grows in village residential areas [20]. People often use bamboo for their needs, such as a fence to protect their gardens from pests, as is done by the people in Nagari Sungai Jambu, Pariangan District, West Sumatra. However, this use will produce waste bamboo pieces even though this waste can be used as a more helpful material. In 2017, Farma et al., used Betung Bamboo as active carbon [21]. Rough bamboo can be used as active carbon by activating

phosphoric acid (H_3PO_4) because it is a weak acid that can produce good-quality activated carbon [22]. The carbon content contained in lignin and cellulose found in rough bamboo makes this material a suitable material to be used as an alternative for making active carbon. Rough bamboo has a cellulose content ranging from 42,4%-53,6%, lignin content 19,8%-26,6%, ash content 1,24%-3,77%, and silica content 0,10%-1,78% [23,24].

Nanotechnology is often used to develop new classes of advanced materials that meet the demands of high-tech applications [25]. One application of nanotechnology is to create nano-sized materials, including nanocomposites [26]. Nanocomposite materials have superior properties compared to larger-sized materials. Nanocomposites are solid structures with nanometer dimensions that repeat between the distances that make up different structures. This material comprises two or more organic/inorganic molecules in the form of several combinations with a barrier between them of at least one molecule or has nano-sized characteristics[27]. Inserting nanoparticles such as activated carbon into macroscopic TiO_2 will produce superior properties compared to previous materials [28]. Therefore, TiO_2 and activated carbon will be made into a TiO_2/Activated carbon nanocomposite to be applied as an energy storage material.

The active carbon material in the TiO_2/Activated carbon nanocomposite will be able to increase the superior properties of the nanocomposite. Activated carbon, which has nanoscale particle size, will have a large surface area and a regular pore structure to store more energy[15], compared to TiO_2 or graphite. Small particle size can affect the ion absorption capacity of a material [12]. The addition of activated carbon to manufacture nanocomposites dramatically influences the properties of the composite [29]. Therefore, the surface area of a material will be an essential factor in determining energy storage capacity. The greater the surface area, the greater the energy storage capacity of the material [15].

The good method for synthesis nanocomposites is by using the sol-gel method [30]. The sol-gel method is based on hydrolysis and condensation reactions under certain conditions that produce hydroxide or oxide compounds [31]. The sol process can be interpreted as forming inorganic compounds through a low-temperature chemical reaction. In this process, a phase change from a colloidal suspension or sol will undergo hydrolysis and condensation to a higher viscosity, forming a gel [32]. This method can operate at low temperatures, has high purity and good solvent resistance, and produces a large surface area or smaller particle sizes [31]. The sol-gel method is divided into sol making, gel formation, aging or ripening, and drying [30]. So, in this research, the synthesis of TiO_2/Rough bamboo activated carbon nanocomposites will be carried out using the sol-gel method. The scheme of sol to gel formation can be seen in Figure 2.

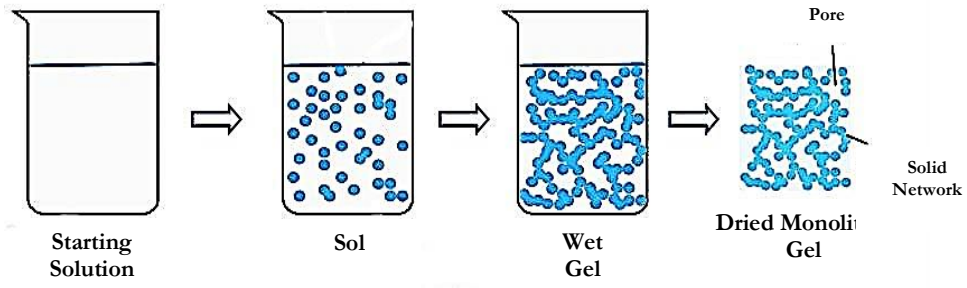

Figure 1. Schematic of sol-gel method [33]

The TiO_2/Rough bamboo activated carbon nanocomposite will be characterized using *X-ray Diffraction* (XRD). XRD is a material characterization method used to identify the crystalline phase in the material [34]. XRD has a working system based on Bragg's Law. This process occurs during X-ray Diffraction, namely the interaction between X-rays and atoms in each crystal plane, resulting in interference in intensity peaks [35]. This characterization can determine the crystal's lattice constant, structure, and size [36].

This research will synthesis nanocomposites with mass variation. So we can see the superior properties of the material used. Based on this explanation, the researcher's questions arise. What are the lattice parameters, structure, and crystal size of the raw carbon, activated carbon, and TiO_2 materials that will be synthesized into nanocomposites?. What are the lattice parameters, structure and crystal size of the TiO_2/Rough bamboo activated carbon nanocomposite?. So, this research aims to determine the lattice constant, structure, and crystal size of carbon, active carbon, and TiO_2. This research also determines the lattice constant, structure, and crystal size of various TiO_2/Rough bamboo activated carbon nanocomposites. The results of the synthesis and characterization of the material will then be used as a reference material in determining the electrical properties of the TiO_2/Rough bamboo activated carbon nanocomposite.

2. Materials and Method

The synthesis of TiO2/Activated carbon nanocomposites begans with manufacturing activated carbon powder. Activated carbon was made through two stages: carbonization and activation [17]. Activated carbon is made based on research conducted by Manurung et al. (2019) [22]. Old rough bamboo is cleaned, dried in the sun until dry, and has a water content of <10%. Water content can be calculated using Equation (1) below [37].

$$\text{Water levels (\%)} = \frac{a-b}{a} \times 100\% \qquad (1)$$

Equation (1) is the equation for the water content of bamboo, "a" is the mass of bamboo before drying (g), and "b" is the mass of bamboo after drying. The bamboo is then carbonized at a temperature of 600°C for 1 hour. Then, the carbon is crushed and sieved. The carbon was then activated using a H_3PO_4 20% solution for 24 hours with a carbon and activator ratio of 6:1. The activated carbon was washed until it reached neutral pH and filtered. The activated carbon was then dried in an oven at 110°C for 6 hours. The activated carbon is milled for 3 hours to achieve nano-size particles and sieved using a 230 mesh sieve [22].

The synthesis of TiO_2/Activated carbon nanocomposites uses the sol-gel method and is based on research conducted by Negara and Astuti (2015) [17]. The raw materials for TiO_2 fiber and activated carbon were prepared with mass variations, namely 40% : 60%, 50% : 50%, and 60% : 40%, with a total mass of 3,2 grams. A total of 45 grams of PEG 6000 was dissolved in 60 mL of ethanol using a Hot Plate Magnetic Stirrer at 50°C. After the solution is homogeneous, variations of TiO_2 powder and activated carbon are added slowly, followed by citric acid until it reaches an acidic pH. The stirring temperature was increased to 100°C, and the stirrer speed was increased to 1000 rpm for 1,5 hours until the gel formed. The gel is then calcined to a temperature of 300°C so that it becomes dry. The gel was then milled for 1 hour to produce a fine nanocomposite powder. Powdered nanocomposites were characterized using XRD to

determine the lattice constant, structure, and size of crystals with certain phases [38]. The crystal structure was determined by standard data fitting [39]. The crystal size is calculated using the Scherrer equation, and the determination refers to the prominent peaks of the diffractogram pattern, namely with Equation (2) below [40].

$$d = \frac{0{,}94\lambda}{\beta cos\theta_{\beta}} \qquad (2)$$

3. Results and Discussion

Carbon and activated carbon are characterized by using XRD, which aims to see the structure and size of the crystals. Another thing is to see whether the activated carbon to be used is active or to see the difference between carbon and activated carbon. The test results can be seen in Figure 2.

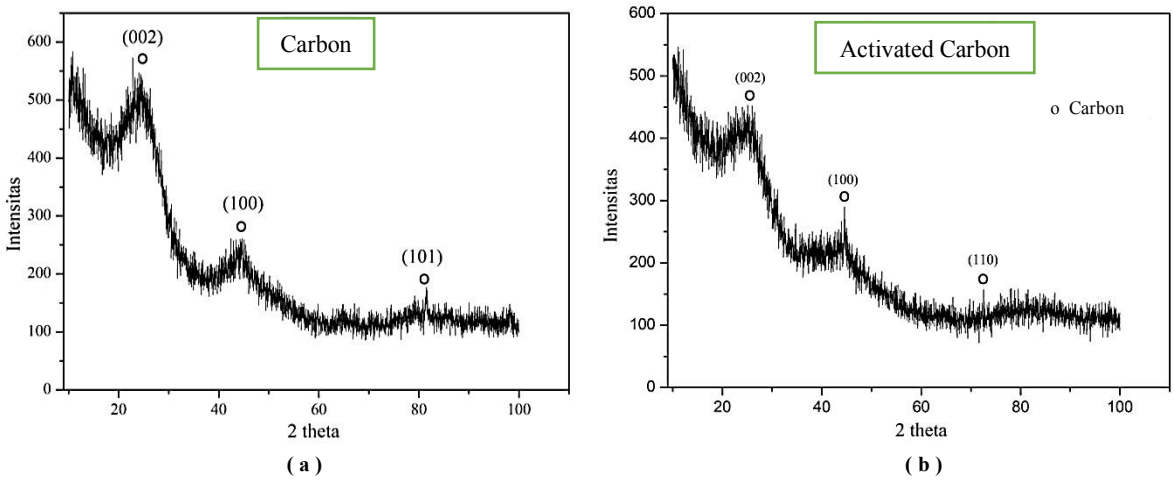

Figure 2. (a) XRD graph of carbon and (b) activated carbon of rough bamboo

The image above shows the relationship between intensity and diffraction angle, with significant intensity peaks at certain angles. It can be seen that active carbon has experienced a decrease in peak; this is because active carbon has a smaller crystal size than carbon material [41] and undergoes changes in structural form [42]. Activated carbon that has undergone an activation process will have a smaller crystal size and more open pores. It affects the material characterization results and causes peak shifts [21,30]. The diffraction pattern measurement data obtained is in Tables 1 and 2.

Table 1. Data for each peaks carbon of rough bamboo

Angle 2θ	h k l	a (Å)	b (Å)	c (Å)	α (°)	β (°)	γ (°)	FWHM	Intensity	Phase	Crystal Structure
29,176	0 0 2	2,46	2,46	6,74	90	90	120	0,1791	53,97	C	Hexagonal
44,550	1 0 0	2,46	2,46	6,74	90	90	120	0,1535	100	C	Hexagonal
86,918	1 0 1	9,53	8,87	8,34	90	90	90	0,1535	52,43	C	Orthorombic

Table 2. Data for each peaks activated carbon of rough bamboo

Angle 2θ	h k l	a (Å)	b (Å)	c (Å)	α (°)	β (°)	γ (°)	FWHM	Intensity	Phase	Crystal Structure
24,415	0 0 2	2,46	4,26	29,0	90	90	90	0,8187	100	C	Orthorombic
44,640	1 0 0	2,47	2,47	6,8	90	90	120	0,2558	56,45	C	Hexagonal
73,684	1 1 0	2,47	2,47	6,8	90	90	120	0,2558	22,21	C	Hexagonal

Based on Tables 1 and 2, it can be seen that carbon and activated carbon only have a carbon phase. Based on the data obtained, carbon has two crystal structures: hexagonal and orthorhombic. Meanwhile, activated carbon has an orthorhombic and hexagonal crystal structure. The lattice parameters obtained are by the specified crystal system. In hexagonal a=b≠c and α=β=90° and γ=120°, the orthorhombic structure is a≠b≠c and α=β=γ=90° [43]. These results have shown a match between the data and the analysis conducted. The height and low of the resulting peak is influenced by the activation process which causes a shift in the hexagonal plate which was originally at a high level of regularity (crystalline) to become irregular (amorphous) as carried out by Farma, et al. [21]. The crystal size can be determined using Equation (2) and can be seen in Tables 3 & 4 below.

Table 3. Rough bambbo carbon crystal size

Material	k	$\lambda\ (nm)$	θ (°)	$\beta\ (rad)$	$D\ (nm)$
Carbon	0,94	0,1546	0,089544	0,001563	88,68473
Carbon	0,94	0,1546	0,076752	0,00134	103,4656
Carbon	0,94	0,1546	0,076752	0,00134	206,9312

Table 4. Rough bamboo activated carbon crystal size

Material	k	$\lambda\ (nm)$	θ (°)	$\beta\ (rad)$	$D\ (nm)$
Activated Carbon	0,94	0,1546	0,409344	0,007144	19,39931
Activated Carbon	0,94	0,1546	0,12792	0,002233	62,07923
Activated Carbon	0,94	0,1546	0,12792	0,002233	62,07923

Based on Tables 3 and 4, carbon material is more significant than active carbon material. Carbon has an average size of 133,03 nm, while activated carbon has a size of 47,85 nm. It is because activated carbon has gone through a carbonization process and is then activated using H_3PO_4. Then, the activated carbon also goes through a grinding process using HEM, resulting in smaller crystal-sized particles.

Another forming material that XRD will characterize is *Titanium dioksida* (TiO_2) to know its lattice constant, structure, and crystal size. So, we can see the differences in the forming materials with variations in the TiO_2/Rough bamboo activated carbon nanocomposite material. The results of TiO_2 characterization can be seen in Figure 3.

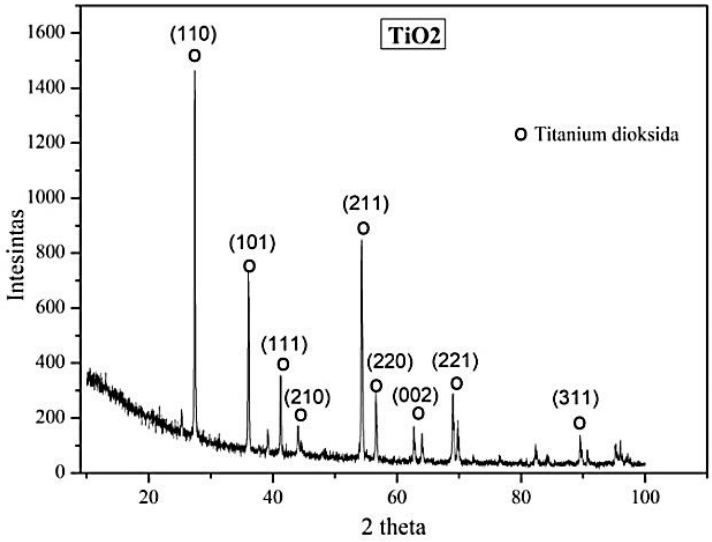

Figure 3. XRD graph of TiO_2

The figure above shows the relationship between intensity and diffraction angle and significant intensity peaks at certain angles. It can be seen that TiO_2 has peak data. The diffraction pattern measurement data obtained is in Table 5.

Table 5. Data for each TiO_2 peak

Angle 2θ	h k l	a (Å)	b (Å)	c (Å)	α (°)	β (°)	γ (°)	FWHM	Intensity	Phase	Crystal Structure
27,442	1 1 0	4,59	4,59	2,96	90	90	90	0,1535	100	TiO_2	Tetragonal
36,063	1 0 1	4,59	4,59	2,96	90	90	90	0,1535	48,5	TiO_2	Tetragonal
41,236	1 1 1	4,59	4,59	2,96	90	90	90	0,1279	20,72	TiO_2	Tetragonal
44,049	2 1 0	4,59	4,59	2,96	90	90	90	0,2047	6,88	TiO_2	Tetragonal
54,293	2 1 1	4,59	4,59	2,96	90	90	90	0,1023	57,04	TiO_2	Tetragonal
56,605	2 2 0	4,59	4,59	2,96	90	90	90	0,1023	17,78	TiO_2	Tetragonal
64,017	0 0 2	4,59	4,59	2,96	90	90	90	0,2047	7,42	TiO_2	Tetragonal
69,763	2 2 1	4,59	4,59	2,96	90	90	90	0,1535	9,34	TiO_2	Tetragonal
89,606	3 1 1	4,59	4,59	2,96	90	90	90	0,4093	4,68	TiO_2	Tetragonal
27,442	1 1 0	4,59	4,59	2,96	90	90	90	0,1535	100	TiO_2	Tetragonal
36,063	1 0 1	4,59	4,59	2,96	90	90	90	0,1535	48,5	TiO_2	Tetragonal
41,236	1 1 1	4,59	4,59	2,96	90	90	90	0,1279	20,72	TiO_2	Tetragonal

Based on Table 5, the highest peak on the graph is at angle of $2\theta = 27{,}4419°$, which has been matched with the PDF 01-086-0147. The TiO_2 material has a tetragonal crystal structure. If it matches the grid parameters, then the data and analysis match. Using Equation (2), we will get the crystal size in Table 6.

Table 6. TiO_2 crystal size

Material	k	$\lambda\ (nm)$	$\theta\ (°)$	$\beta\ (rad)$	$D\ (nm)$
TiO_2	0,94	0,1546	0,076752	0,00134	103,4656
TiO_2	0,94	0,1546	0,076752	0,00134	103,4656
TiO_2	0,94	0,1546	0,06396	0,001116	124,1587
TiO_2	0,94	0,1546	0,102336	0,001786	77,59911
TiO_2	0,94	0,1546	0,051168	0,000893	155,1984
TiO_2	0,94	0,1546	0,051168	0,000893	155,1984
TiO_2	0,94	0,1546	0,102336	0,001786	77,59911
TiO_2	0,94	0,1546	0,076752	0,00134	103,4656
TiO_2	0,94	0,1546	0,204672	0,003572	38,79937
TiO_2	0,94	0,1546	0,076752	0,00134	103,4656
TiO_2	0,94	0,1546	0,076752	0,00134	103,4656
TiO_2	0,94	0,1546	0,06396	0,001116	124,1587

Based on the table above, it can be seen that TiO2 has an average size of 98.477 nm. This material has a larger crystal size than activated carbon.

Furthermore, the forming materials, such as activated carbon and TiO2, will be made into TiO_2/Rough bamboo activated carbon nanocomposites. The nanocomposite was synthesized using the sol-gel method. The variations carried out were in the mass ratio of TiO_2 to activated carbon, namely 40% : 60%, 50% : 50%, and 60% : 40%. It aims to see the superior properties of each material used. Each nanocomposite variation was characterized using XRD to see lattice constants, structure, and crystal size. The results of the characterization of each variation can be seen in Figure 4.

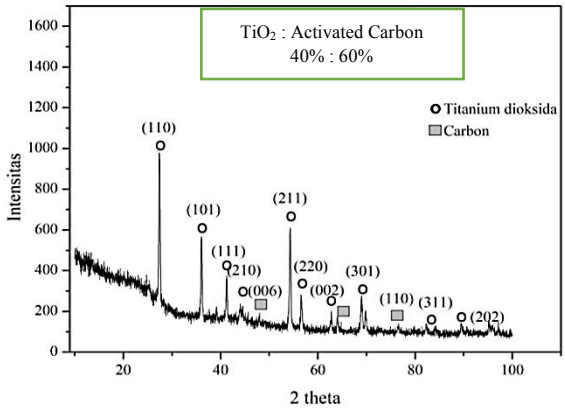

(a)

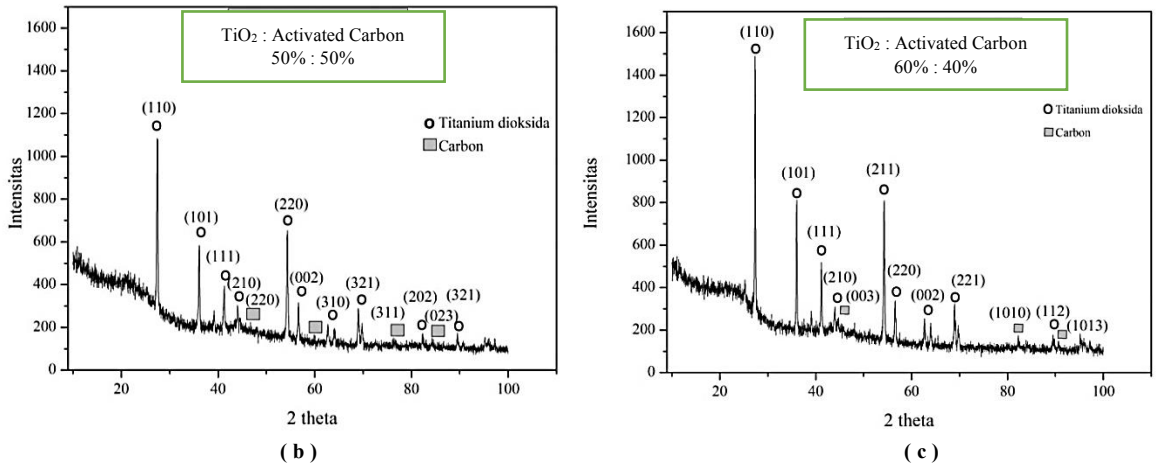

Figure 4. XRD graph with variation of (a) 40% : 60%, (b) 50% : 50%, and (c) 60% : 40%

Based on Figure 4 above, it can be seen that each variation experiences a decline and peak shift. It is because each variation has a different composition of TiO_2 and activated carbon and a different crystal form. The TiO_2 and active carbon content affect the grain size of each nanocomposite variation. It is because if we look at the results, activated carbon has a smaller crystal size than TiO_2. So, if the more TiO_2 mass is added, the more significant the increase in the highest peak value. Moreover, the nanocomposite particle size will be smaller if more activated carbon is added. The 40% : 60% variation has the minor peak because it has the most negligible TiO_2 mass, while the 60% : 40% variation has the highest peak because it has the most TiO_2. This nanocomposite has only 2 phases, namely the *Titanium dioxide* (TiO_2) and the carbon (C) phase.

To determine the crystal system of each variation, PDF data is matched between the lattice parameters and the crystal system obtained. Data for each peak of the nanocomposite variation of 40% : 60% can be seen in Table 7 below.

Table 7. Data for each TiO_2/Activated carbon nanocomposite peak varies 40% : 60%

Angle 2θ	h k l	a (Å)	b (Å)	c (Å)	α (°)	β (°)	γ (°)	FWHM	Intensity	Phase	Crystal Structure
27,397	1 1 0	4,60	4,60	2,96	90	90	90	0,2047	100	TiO_2	Tetragonal
36,039	1 0 1	4,60	4,60	2,96	90	90	90	0,1791	53,33	TiO_2	Tetragonal
39,187	1 1 1	4,60	4,60	2,96	90	90	90	0,3070	6,49	TiO_2	Tetragonal
41,266	2 1 0	4,60	4,60	2,96	90	90	90	0,2558	26,7	TiO_2	Tetragonal
44,014	0 0 3	2,52	2,52	4,12	90	90	120	0,3070	9,86	C	Hexagonal
54,301	2 1 1	4,60	4,60	2,96	90	90	90	0,1535	66,95	TiO_2	Tetragonal
56,578	2 2 0	4,60	4,60	2,96	90	90	90	0,2558	24,24	TiO_2	Tetragonal
62,741	0 0 2	4,60	4,60	2,96	90	90	90	0,4093	10,54	TiO_2	Tetragonal
63,994	2 2 1	4,60	4,60	2,96	90	90	90	0,2558	9,56	TiO_2	Tetragonal
68,980	1 0 1	2,52	2,52	4,12	90	90	120	0,3582	23,72	C	Hexagonal
69,780	1 1 2	4,60	4,60	2,96	90	90	90	0,2047	13,89	TiO_2	Tetragonal
82,314	1 0 3	2,52	2,52	4,12	90	90	120	0,3070	7,28	C	Hexagonal

Based on Table 7 above, we can see the highest peak of variation of 40% : 60%, namely at angle of 2θ=27,3971°. This variation has 2 phases, namely, the TiO_2 phase and the C phase. Suppose we compare the lattice parameters and the crystal system. In that case, it is found that in this variation, there are two crystal systems, namely tetragonal and hexagonal, where the tetragonal parameters are a=b≠c dan α=β=γ= 90°. In contrast, the hexagonal parameters are a=b≠c dan α=β= 90° & γ= 120° [43]. To find out the crystal size, by using Equation (2), the data in Table 8 will be obtained.

Table 8. Crystal size variation 40% : 60%

Material	k	$\lambda\ (nm)$	$\theta\ (°)$	$\beta\ (rad)$	$D\ (nm)$
TiO_2	0,001786	0,102336	0,001786	0,102336	77,59936
TiO_2	0,001563	0,089544	0,001563	0,089544	88,68495
TiO_2	0,002679	0,153504	0,002679	0,153504	51,73301
TiO_2	0,002233	0,12792	0,002233	0,12792	62,07954
C	0,002679	0,153504	0,002679	0,153504	51,73301
TiO_2	0,00134	0,076752	0,00134	0,076752	103,4657
TiO_2	0,002233	0,12792	0,002233	0,12792	62,07954
TiO_2	0,003572	0,204672	0,003572	0,204672	38,79986
TiO_2	0,002233	0,12792	0,002233	0,12792	62,07954
C	0,003126	0,179088	0,003126	0,179088	44,34264
TiO_2	0,001786	0,102336	0,001786	0,102336	77,59936
C	0,002679	0,153504	0,002679	0,153504	51,73301

Based on Table 8 above, it can be seen that this variation has an average crystal size of 64,3275 nm. This material meets the requirements of a nanocomposite, namely having a size below 100 nm [44]. Data for each peak with a variation of 50% : 50% is in Table 9 below.

Table 9. Data for each TiO_2/Activated carbon nanocomposite peak varies 50% : 50%

Angle 2θ	h k l	a (Å)	b (Å)	c (Å)	α (°)	β (°)	γ (°)	FWHM	Intensity	Phase	Crystal Structure
27,512	1 1 0	4,59	4,59	2,96	90	90	90	0,2047	100	TiO_2	Tetragonal
36,131	1 0 1	4,59	4,59	2,96	90	90	90	0,2047	44,5	TiO_2	Tetragonal
41,232	1 1 1	4,59	4,59	2,96	90	90	90	0,1791	24,17	TiO_2	Tetragonal
44,112	2 1 0	4,59	4,59	2,96	90	90	90	0,2047	12,79	TiO_2	Tetragonal
39,202	2 2 0	11,9	11,9	10,6	90	90	120	0,2558	7,08	C	Hexagonal
54,368	2 2 0	4,59	4,59	2,96	90	90	90	0,2047	64,49	TiO_2	Tetragonal
56,608	0 0 2	11,9	11,9	10,6	90	90	120	0,2047	20,31	TiO_2	Tetragonal
64,079	3 1 0	4,59	4,59	2,96	90	90	90	0,3070	6,28	TiO_2	Tetragonal
68,995	3 2 1	4,59	4,59	2,96	90	90	90	0,2558	21,14	TiO_2	Tetragonal
78,995	0 2 3	11,9	11,9	10,6	90	90	120	0,1535	2,47	C	Hexagonal
78,084	2 0 2	4,59	4,59	2,96	90	90	90	0,3070	6,39	TiO_2	Tetragonal
95,237	3 2 1	4,59	4,59	2,96	90	90	90	0,3070	6,44	TiO_2	Tetragonal

Based on Table 9 above, we can see the highest peak of variation of 50% : 50%, namely at angle of 2θ=27,512°. The peak has shifted when compared with a variation of 40% : 60%. It is due to the different amounts of TiO_2 and activated carbon. So that it affects the XRD characterization results. This variation has 2 phases, namely, the TiO_2 phase and the C phase. If we compare the lattice parameters and the crystal system, it is found that in this variation, there are two crystal systems, namely tetragonal and hexagonal. The tetragonal parameters are a=b≠c dan α=β=γ= 90°, while the hexagonal parameters are a=b≠c dan α=β= 90° & γ= 120° [43]. To find out the crystal size, by using Equation (2), we will get the crystal size in Table 10.

Table 10. Crystal size variation 50% : 50%

Material	k	$\lambda\ (nm)$	$\theta\ (°)$	$\beta\ (rad)$	$D\ (nm)$
TiO_2	0,94	0,1546	0,102336	0,001786	77,59936
TiO_2	0,94	0,1546	0,102336	0,001786	77,59936
TiO_2	0,94	0,1546	0,089544	0,001563	88,68495
TiO_2	0,94	0,1546	0,102336	0,001786	77,59936
C	0,94	0,1546	0,12792	0,002233	62,07923
TiO_2	0,94	0,1546	0,102336	0,001786	77,59936
TiO_2	0,94	0,1546	0,102336	0,001786	77,59936
TiO_2	0,94	0,1546	0,204672	0,003572	38,79986
TiO_2	0,94	0,1546	0,12792	0,002233	62,07954
C	0,94	0,1546	0,076752	0,00134	103,4656
TiO_2	0,94	0,1546	0,153504	0,002679	51,73301
TiO_2	0,94	0,1546	0,153504	0,002679	51,73301

In Table 10, the crystal size in the 50% : 50% variation has an average crystal size value of 70.54762 nm. The nanocomposite has a larger crystal size than the 40%: 60% variation in this variation. It is because the addition of TiO2 can affect the crystal size. Data for each peak at a variation of 60%: 40% can be seen in Table 11.

Table 11. Data for each TiO_2/Activated carbon nanocomposite peak varies 60% : 40%

Angle 2θ	h k l	a (Å)	b (Å)	c (Å)	α (°)	β (°)	γ (°)	FWHM	Intensity	Phase	Crystal Structure
27,383	1 1 0	4,60	4,60	2,96	90	90	90	0,1535	100	TiO_2	Tetragonal
35,999	1 0 1	4,60	4,60	2,96	90	90	90	0,1791	48,07	TiO_2	Tetragonal
41,180	1 1 1	4,60	4,60	2,96	90	90	90	0,1023	22,82	TiO_2	Tetragonal
43,976	2 1 0	4,60	4,60	2,96	90	90	90	0,2047	7,81	TiO_2	Tetragonal
44,053	0 0 6	2,52	2,52	43,2	90	90	120	0,3070	9,63	C	Rhombo hedral
54,253	2 1 1	4,60	4,60	2,96	90	90	90	0,1279	54,15	TiO_2	Tetragonal
64,017	2 2 0	2,52	2,52	43,2	90	90	120	0,1279	9,06	C	Rhombo hedral

62,655	0 0 2	4,60	4,60	2,96	90	90	90	0,2047	9,19	TiO_2	Tetragonal
76,659	3 0 1	2,52	2,52	43,2	90	90	120	0,3582	2,94	C	Rhombo hedral
68,954	1 1 0	4,60	4,60	2,96	90	90	90	0,2047	15,93	TiO_2	Tetragonal
89,573	3 1 1	4,60	4,60	2,96	90	90	90	0,2047	3,22	TiO_2	Tetragonal
95,243	2 0 2	4,60	4,60	2,96	90	90	90	0,2047	3,23	TiO_2	Tetragonal

Based on Table 11 above, we can see the highest peak of variation of 60% : 40%, namely at angle of 2θ=27,3830°. The peak has shifted when compared with variations of 40% : 60% and 50% : 50%. It is due to the different amounts of TiO_2 and activated carbon. So that it affects the XRD characterization results. This variation has 2 phases, namely, the TiO_2 phase and the C phase. If we compare the lattice parameters and the crystal system, it is found that in this variation, there are two crystal systems, namely tetragonal and rhombohedral. The tetragonal parameters are a=b≠c dan α=β=γ=90°, while the hexagonal parameters are a=b≠c dan α=β=90° & γ= 120° [43]. To find out the crystal size, by using Equation (2), we will get the crystal size in Table 12 below.

Table 12. Crystal size variation 60% : 40%

Material	k	$\lambda\ (nm)$	θ (°)	$\beta\ (rad)$	$D\ (nm)$
TiO_2	0,94	0,1546	0,076752	0,00134	103,4657
TiO_2	0,94	0,1546	0,089544	0,001563	88,68495
TiO_2	0,94	0,1546	0,051168	0,000893	155,1985
TiO_2	0,94	0,1546	0,102336	0,001786	77,59936
C	0,94	0,1546	0,153504	0,002679	51,73264
TiO_2	0,94	0,1546	0,06396	0,001116	124,1588
C	0,94	0,1546	0,06396	0,001116	124,1587
TiO_2	0,94	0,1546	0,102336	0,001786	123,1588
C	0,94	0,1546	0,179088	0,003126	38,79937
TiO_2	0,94	0,1546	0,089544	0,001563	88,68495
TiO_2	0,94	0,1546	0,307008	0,005358	25,86678
TiO_2	0,94	0,1546	0,204672	0,003572	38,79986

Based on the analysis results in Table 12, it can be seen that this variation has an average crystal size of 86,6924 nm. Compared to other variations, this variation has the most significant crystal size. It is because the variation of 60% : 40% has the highest mass of TiO_2, thus affecting the crystal size of the nanocomposite material. Based on the table above, it can be seen that the 40% : 60% variation has the smallest crystal size because it has the highest active carbon content. Activated carbon has a smaller particle size than TiO_2, so the material with the highest carbon content will have the smallest particle size. Meanwhile, the 60% : 40% variation has the most significant crystal size because it has the highest TiO_2 content. The XRD intensity value is influenced by the material's crystallinity level, where the higher the intensity, the more crystalline the material. When a material has a crystalline structure, the atomic arrangement will be more orderly and neat [45]. It is what can affect the properties of the material itself, including its

electrical properties. When the atomic arrangement becomes neater, electrons will flow more quickly in the material and give the material better conductivity properties [46]. If seen from the results of this research, nanocomposites have a crystal size below 100 nm and meet the requirements for nanocomposite materials [44]. Judging from the research results, nanocomposites can be further analyzed for their electrical properties such as electrical conductivity and specific capacitance, so that they can be applied as anode materials for rechargeable batteries like lithium ion battery.

4. Conclusion

Synthesis of TiO_2/Activated carbon nanocomposites has been successfully created. Results of analysis of lattice parameters, structure, and crystal size of the forming materials: carbon, activated carbon, and TiO_2. The lattice parameters of carbon and activated carbon determine their crystal structures, namely hexagonal and orthorhombic. The crystal size of carbon is 133,03 nm, and active carbon is 47,85 nm. Activated carbon is smaller because it has gone through a carbonization, activation, and grinding process. Another forming material, namely TiO_2, has a tetragonal crystal structure with lattice parameters a=b=4,59 Å dan $\alpha=\beta=\gamma=90°$. TiO_2 has a crystal size of 98,477 nm. The TiO_2/Rough bamboo activated carbon nanocomposite has been successfully synthesized using the sol-gel method and has fulfilled the requirements as a nanocomposite. In the 40% : 60% variation, with the existing lattice parameters, this variation has a crystal structure in the form of tetragonal and hexagonal with a particle size of 64,3275 nm. Variation 50% : 50% has a tetragonal and hexagonal crystal structure with a particle size of 70,54762 nm. With 60% : 40% variations, the lattice parameters have been obtained so that the lattice structure is tetragonal and rhombohedral, with a crystal size of 86,6924 nm. Among the three variations, the 40% : 60% variation has the smallest crystal size because it has the highest active carbon content. Meanwhile, the 60%: 40% variation has the most significant crystal size because it has the highest TiO_2 content. So, the more active carbon added, the smaller the crystal size. Moreover, the more TiO_2 is added, the larger the crystal size of the material will be. It is because activated carbon has a smaller crystal size than TiO_2. With the success of this nanocomposite material, it will then be able to be applied to battery anode materials or analyze its electrical properties.

Acknowledgments

The author would like to thank the supervisors who assisted in conducting this research and is also grateful to parents, family, and friends who have supported the author.

References

[1] T. Nusa, "Sistem Monitoring Konsumsi Energi Listrik Secara Real Time Berbasis Mikrokontroler," *E-journal Tek. Elektro dan Komput.*, vol. 4, no. 5, pp. 19–26, 2015.

[2] F. Lamablawa and S. Aritonang, "Karakteristik Lithium-Polymer Battery Untuk Aplikasi Radio Yang Di Gunakan Personil Tni Dalam Mendukung Ikn Literature Review," *Citiz. J. Ilm. Multidisiplin Indones.*, vol. 2, no. 4, pp. 592–602, 2022.

[3] I. D. A. F. Antika and S. Hidayat, "Karakteristik Anoda Baterai Lithium-Ion yang Dibuat

dengan Metode SPraying Berbasis Binder CMC," *J. Ilmu dan Inov. Fis.*, vol. 03, no. 02, pp. 114–121, 2019.

[4] F. A. Perdana, "Baterai Lithium," *INKUIRI J. Pendidik. IPA*, vol. 9, no. 2, p. 113, 2021.

[5] Deswita and I. Gunawan, "Analisis dan Karakterisasi Bahan Standar Anoda, Katoda dan Separator Sebagai Komponen Baterai Lithium Ion," *Pros. Semin. Nas. XXV "Kimia dalam Ind. dan Lingkungan,"* 2016.

[6] A. Aflahannisa and A. Astuti, "Sintesis Nanokomposit Karbon-TiO2 Sebagai Anoda Baterai Lithium," *J. Fis. Unand*, vol. 5, no. 4, pp. 357–363, 2016.

[7] J. Ginting, E. Yulianti, and Sudaryanto, "Sintesis Li2TiO3 Sebagai Bahan Anoda Baterai Li-ion degan Metode Reaksi Padatan," *J. Sains Mater. Indones.*, vol. 15, no. 4, pp. 196–200, 2014.

[8] S. Priyono, M. A. Dhika, K. Sebayang, and A. Subhan, "Pembuatan Anoda Li4Ti5O12 dan Studi Pengaruh Ketebalan Elektroda terhadap Performa Elektrokimia Baterai Ion Lithium," *Indones. J. …*, vol. 17, no. 4, pp. 3–9, 2016.

[9] C. Zhao, L. Liu, Q. Zhang, J. Rogers, H. Zhao, and Y. Li, "Synthesis of Carbon-TiO2 nanocomposites with enhanced reversible capacity and cyclic performance as anodes for lithium-ion batteries," *Electrochim. Acta*, vol. 155, pp. 288–296, 2015.

[10] I. M. I. M. Brunner and S. M. Brunner, "Pemilihan Baterai Kendaraan Listrik dengan Metoda Weighted Objective," *J. Serambi Eng.*, vol. 6, no. 1, pp. 1563–1572, 2021.

[11] S. Goriparti, E. Miele, F. De Angelis, E. Di Fabrizio, R. Proietti Zaccaria, and C. Capiglia, "Review on recent progress of nanostructured anode materials for Li-ion batteries," *J. Power Sources*, vol. 257, pp. 421–443, 2014.

[12] Y. Arsita and A. Astuti, "Sintesis Komposit TiO2/Karbon Aktif Berbasis Bambu Betung (Dendrocalamus asper) dengan Menggunakan Metode Solid State Reaction," *J. Fis. Unand*, vol. 5, no. 3, pp. 268–272, 2016.

[13] L. Maulinda, Z. Nasrul, and D. N. Sari, "Jurnal Teknologi Kimia Unimal Pemanfaatan Kulit Singkong sebagai Bahan Baku Karbon Aktif," *J. Teknol. Kim. Unimal*, vol. 4, no. 2, pp. 11–19, 2015.

[14] A. Li *et al.*, "A Review on Lithium-Ion Battery Separators towards Enhanced Safety Performances and Modelling Approaches," *Molecules*, vol. 26, no. 478, p. 26020478, 2021.

[15] M. Rosi, F. Iskandar, and M. Abdullah, "Sintesis Nanopori Karbon dengan Variasi Jumlah NaOH dan Aplikasinya sebagai Superkapasitor Sintesis Nanopori Karbon dengan Variasi Jumlah NaOH dan Aplikasinya sebagai Superkapasitor," *Semin. Nas. Fis. Inst. Teknol. Bandung*, pp. 74–77, 2013.

[16] A. M. Taspika, "Pembuatan Elektroda Kapasitor Karbon Berpori Dari Tempurung Kemiri (Aleurites Moluccana) Sebagai Sistem Capacitive Deionization," *J. Fis. Unand*, vol. 4, no. 2, pp. 173–177, 2015.

[17] V. S. I. Negara and Astuti, *Pengaruh Temperatur Sintering Karbon Aktif Berbasis Tempurung Kemiri Terhadap Sifat Listrik Anoda Baterai Litium*, vol. 4, no. 2. 2015.

[18] H. Susana and Astuti, "Pengaruh Konsentrasi LiOH terhadap Sifat Listrik Anoda Baterai Litium Berbasis Karbon Aktif Tempurung Kemiri," *J. Fis. Unand*, vol. 5, no. 2, pp. 136–141, 2016.

[19] L. Amaranggana and N. Wathoni, "Manfaat Alga Merah (Rhodophyta) Sebagai Sumber Obat dari Bahan Alam," *Farmasetika.com (Online)*, vol. 2, no. 1, p. 16, 2017.

[20] M. K. Allo, "Aspek Fisik Lingkungan Bagi Peningkatan Produksi Rebung Bambu Petung (Dendrocalamus asper) sebagai Pangan Eksklusif," *Pros. Semin. Nas. Fak. Pertan. Univ. Sebel. Maret*, vol. 2, no. 1, pp. 29–41, 2018.

[21] R. Farma, Saktioto, and Awitdrus, "Pembuatan dan karakterisasi karbon aktifdari bambu betung (Dendrocalamus asper) dengan aktivasi KOH berbantuan gelombang mikro," *J. Komun. Fis. Indones.*, vol. 14, no. 02, pp. 1–6, 2017.

[22] M. Manurung, E. Sahara, and S. Sihombing, "Pembuatan dan Karakterisasi Arang Aktif dari Bambu Apus (Gigantochloa apus) dengan Aktivator H_3PO_4," *J. Chem.*, vol. 13, 2019.

[23] Krisdianto, G. Sumarni, and A. Ismanto, *Sari Hasil Penelitian Bambu*. 2000.

[24] K. K. H. Choy, J. P. Barford, and G. McKay, "Production of activated carbon from bamboo scaffolding waste - Process design, evaluation and sensitivity analysis," *Chem. Eng. J.*, vol. 109, no. 1, pp. 147–165, 2005.

[25] I. A. Rahman and V. Padavettan, "Synthesis of Silica nanoparticles by Sol-Gel: Size-dependent properties, surface modification, and applications in silica-polymer nanocompositesa review," *J. Nanomater.*, vol. 2012, 2012.

[26] A. M. Nursanti, A. Syafira, and Priyono, "Studi Literatur: Perkembangan Nanomaterial," *J. Berk. Fis.*, vol. 25, no. 3, 2022.

[27] Hadiyawarman, A. Rijal, B. W. Nuryadin, M. Abdulllah, and Khairurrijal, "Fabrikasi Material Nanokomposit Superkuat, Ringan dan Transparan Menggunakan Metode Simple Mixing," vol. 1, no. 1, pp. 14–21, 2008.

[28] Y. Suyono, "Studi Awal Pembuatan Nanokomposit dengan Filler Organoclay Untuk Kemasan," *Biopropal Ind.*, vol. 3, no. 2, pp. 63–69, 2012.

[29] S. Fu, F. Li, Z. Huo, and Y. Gu, "Effects of the incorporation of carbon spheres into nanostructured TiO2 film for dye-sensitized solar cell," *Int. J. Phys. Sci.*, vol. 6, no. 26, pp. 6159–6165, 2011.

[30] Y. M. Liza, R. C. Yasin, S. S. Maidani, and R. Zainul, "Gelation Sol- Gel Proces s Densification Ageing Drying," *Ina. Pap.*, pp. 1–19, 2018.

[31] H. Khusyaeri and A. Nur, "Studi Komparatif Tentang Metode Sintesis Katoda NCA untuk Baterai Litium Ion," no. October, 2019.

[32] N. P. Trisnayanti, "Metode sintesis nanopartikel," *Univ. Indones.*, no. 3, pp. 1–4, 2020.

[33] A. Feinle, "Sol-gel synthesis of monolithic materials with hierarchical porosity," *AIChE Annu. Meet. Conf. Proc.*, vol. 2019-Novem, 2019.

[34] R. Sharma, D. P. Bisen, U. Shukla, and B. G. Sharma, "X-ray diffraction: a powerful method of characterizing nanomaterials," *Recent Res. Sci. Technol.*, vol. 4, no. 8, pp. 77–79, 2012.

[35] A. A. Bunaciu, E. gabriela Udriştioiu, and H. Y. Aboul-Enein, "X-Ray Diffraction: Instrumentation and Applications," *Crit. Rev. Anal. Chem.*, vol. 45, no. 4, pp. 289–299, 2015.

[36] U. N. Yogyakarta, "Oleh: Risma Widayati, Universitas Negeri Yogyakarta," vol. 2, pp. 261–266, 2011.

[37] M. I. Sari, M. G. Markasiwi, and R. W. Putri, "Uji Karakteristik Fisik Pembuatan Karbon Aktif dari Limbah Daun Nanas (Ananas comosus) Menggunakan Aktivator H_3PO_4," *J. Tek. Patra Akad.*, vol. 12, no. 02, pp. 4–11, 2021.

[38] M. E. Wieser and T. B. Coplen, *Atomic weights of the elements 2009 (IUPAC technical report)*, vol. 83, no. 2. 2011.

[39] T. W. Purnomo, A. Penentuan, S. Kristal, D. Komposisi, K. Lapisan, and T. Sn, "Penentuan Struktur Kristal dan Komposisi Kimia Lapisan Tipis Sn(Se 0,5 S 0,5) Hasil Preparasi Teknik Evaporasi untuk Aplikasi Sel Surya Determination Crystal Structure and Chemical Composition of Sn(Se 0,5 S 0,5) Thin Film from Preparation's Result of E," vol. 15, no. 1, pp. 22–27, 2015.

[40] Masruroh, A. Manggara, T. Papilaka, and R. T. T, "Penentuan ukuran Kristal (crytallite size) lapisan tipis PZT melalui pendekatan persamaan Debye Scherrer," *Jur. Fis. dan Kim. FMIPA Univ. Brawijaya*, vol. 1, no. 2, pp. 24–29, 2013.

[41] M. S. Anggraini, Ramli, and Hidayati, "Pillar of Physics, Vol. 10. Oktober 2017, 47-54," *Pillar Phys.*, vol. 10, pp. 47–54, 2017.

[42] M. Ali, "Qualitative analyses of thin film-based materials validating new structures of atoms," *Mater. Today Commun.*, vol. 36, no. May, 2023.

[43] B. Alam, P. Frekuensi, and A. A. Usman, "Penyerap Gelombang Radar Mikrokomposit rGO-Fe_3O_4," 2019.

[44] M. Marpaung, U. Ahmad, and N. Edhi S, "Edible Coating Nanocomposites to Maintain Quality of Minimally-Processed Snake Fruit," *J. Keteknikan Pertan.*, vol. 03, no. 1, pp. 73–80, 2015.

[45] A. Dwi Ardianti, "Analisis Morfologi dan Struktur Karbon Aktif Kulit Salak Wedi dengan Aktivator Bertingkat," *J. Ilmu dan Inov. Fis.*, vol. 6, no. 1, pp. 53–60, 2022.

[46] R. F. Suwandana and D. Susanti, "Analisis Pengaruh Massa Reduktor Zinc Terhadap Sifat Kapasitif Superkapasitor Material Graphene," *J. Tek. ITS*, vol. 4, no. 1, pp. 95–100, 2015.